

# Peripheral compression as a function of stimulus level and frequency region in normal-hearing listeners

David A. Nelson<sup>a)</sup> and Anna C. Schroder

*Clinical Psychoacoustics Laboratory, Department of Otolaryngology, University of Minnesota, Minneapolis, Minnesota 55455*

(Received 6 April 2003; revised 22 January 2004; accepted 26 January 2004)

Fixed-probe-level temporal masking curves (TMCs) were obtained from normal-hearing listeners at probe frequencies between 250 and 8000 Hz. The short probe tones were fixed in level ( $\sim 10$ -dB SPL). The level of the preceding forward masker was adjusted to obtain masked threshold as a function of the time delay between masker and probe. These *isoresponse* TMCs were obtained for an on-frequency masker, where the masker frequency ( $F_m$ ) and probe frequency ( $F_p$ ) were the same, and for an off-frequency masker below the probe frequency ( $F_m = 0.6F_p$ ). Slopes of off-frequency TMCs for probe tones at 250–1000 Hz were steeper than those for probe tones between 2000 and 4000 Hz, supporting the notion that response growth for  $F_m = 0.6F_p$  at lower probe frequencies is not linear. Therefore, a group average off-frequency TMC slope, for probe frequencies between 2 and 4 kHz, was used to calculate response growth at every probe frequency. Input/output response growth curves were derived from the TMCs, and response growth rates were calculated as a function of the masker level in individual ears. At any particular probe frequency, response growth rates varied with input level, from near 1.0 at low input levels, to  $<0.2$  at mid levels, and back to near 1.0 at levels above 80-dB SPL. It was concluded that compression is equally strong at low and high frequencies as it is at mid frequencies. © 2004 Acoustical Society of America.

[DOI: 10.1121/1.1689341]

PACS numbers: 43.66.Ba, 43.66.Dc, 43.66.Mk [NFV]

Pages: 2221–2233

## I. INTRODUCTION

The normal auditory system exhibits strong nonlinearities that are associated with excellent sensitivity and sharp tuning. These nonlinearities are thought to originate in the outer hair cells of the cochlear partition. Physiological measures indicate that strong nonlinearities exist in basilar membrane motion (Rhode and Robles, 1974; Robles *et al.*, 1986; Murugasu and Russell, 1995; Ruggero *et al.*, 1997; Russell and Nilsen, 1997; Rhode and Recio, 2000) as well as in the growth of the neural response (Yates, 1990; Yates *et al.*, 1990; Cooper and Yates, 1994). These nonlinearities appear to vary with position along the cochlear partition, with stronger nonlinearities in the base of the cochlea, which is excited most easily by high frequencies, than in the apex of the cochlea, which is sensitive to low frequencies. Although very few direct measurements of basilar membrane motion have been made in the apex (Cooper and Rhode, 1995; Rhode and Cooper, 1996; Khanna and Hao, 1999; Zinn *et al.*, 2000), inferences from neural responses suggest that the nonlinearities in the apex are less strong (Cooper and Yates, 1994). Psychophysical evidence also suggests that cochlear nonlinearities are dependent upon the frequency region at which they are measured (for review, see Hicks and Bacon, 1999a). Some of that evidence includes attempts to specify response growth rates from slopes of nonsimultaneous masking growth functions (Moore *et al.*, 1999; Hicks and Bacon,

1999a; Hicks and Bacon, 1999b; Plack and Oxenham, 2000). The results suggest that response growth rates are dependent upon the frequency region in the cochlea, with steeper growth rates reflecting nonlinearities that are less strong at lower characteristic frequencies.

Nelson *et al.* (2001) demonstrated that the slope-ratio procedure, based on forward-masking growth functions obtained in quiet, may be influenced by the spread of excitation toward higher frequencies. The influence can be greater for an off-frequency masker than for an on-frequency masker. Furthermore, the effects of that spread of excitation may vary with frequency region. Consequently, Nelson *et al.* developed a new procedure for estimating response growth from isoresponse Temporal Masking Curves (TMCs),<sup>1</sup> which they demonstrated, are not significantly affected by the spread of excitation toward higher-frequency regions. TMCs describe the masker levels required to just forward mask a fixed-level probe tone as a function of the time delay between the masker and the probe (Nelson and Freyman, 1987). The TMC requires a constant response at the output of an auditory filter, which produces a constant amount of forward-masked threshold shift (masking) at the probe frequency. The input level to that filter is adjusted to maintain the required response as a function of the time delay between the masker and probe. A fixed-level probe tone is chosen at some frequency and the masker level, at some masker frequency, is adjusted until sufficient forward masking is produced to just mask the probe. As time delay is increased, the amount of forward masking decreases, therefore the masker level (input to the auditory filter) must be increased to maintain the same amount of forward masking. The procedure derives input/

<sup>a)</sup>Send correspondence to David A. Nelson, Ph.D., U/M Clinical Psychoacoustics Lab., 38286 Kost Trail, North Branch, Minnesota 55056-6793. Phone: (651) 674-4224; fax: (651) 674-4224; electronic mail: dan@umn.edu

output response growth curves from the slopes of TMCs for off-frequency and on-frequency maskers. Response growth rates and compression exponents are then calculated from those input/output curves, as a function of masker level.

The rationale behind their procedure is as follows: The masker level required to forward mask a probe tone with an *on-frequency masker* ( $F_m = F_p$ ), depends both upon the recovery from forward masking that occurs at the probe-frequency place *and* upon the peripheral compression that exists at the probe-frequency place. By way of contrast, the masker level required to forward mask a probe tone with an *off-frequency masker* ( $F_m \leq 0.6F_p$ ) depends *only* upon the recovery from forward masking that occurs at the probe-frequency place. This is because the off-frequency masker, which is nearly an octave below the probe frequency, presumably has a linear response at the probe-frequency place in the cochlea (Yates, 1990; Yates *et al.*, 1990; Ruggero, 1992; Nelson and Schroder, 1997; Oxenham and Plack, 1997; Ruggero *et al.*, 1997; Moore and Oxenham, 1998; Rhode and Recio, 2000). Therefore, the ratio of the recovery slopes for the off-frequency masker and the on-frequency masker, given the same change in time delay, reflects the additional masker level required in the on-frequency case to overcome cochlear compression and produce the same amount of forward masking. Thus, the ratio of masker level changes for off-frequency and on-frequency maskers as a function of time delay, provides an estimate of response growth at the probe frequency, which is governed by cochlear compression. A critical assumption for this method of estimating compression is that the response to an off-frequency masker is linear at the probe frequency place. Recently, that assumption has been questioned. Forward masking results that did not rely on this assumption suggest that compression is relatively independent of frequency region (Lopez-Poveda *et al.*, 2003; Plack and Drga, 2003; Plack and O'Hanlon, 2003).

The purpose of this study was to evaluate the dependence of off-frequency TMC slopes on probe frequency region, to obtain compression estimates at different frequency regions using the Nelson *et al.* (2001) procedure, and to compare those estimates with previous psychophysical estimates of peripheral nonlinearity.

## II. METHODS

TMCs were obtained for a masker frequency at ( $F_m = F_p$ ) and below ( $F_m = 0.6F_p$ ) a probe frequency. Probe frequencies were 250, 500, 750, 1000, 2000, 3000, 4000, 6000, or 8000 Hz. Masker and probe durations were 200 and 20 ms at peak amplitude, respectively. All stimuli had 10 ms raised-cosine rise and decay times. During each test session, delay times (between masker offset and probe offset) were tested in the following order: 42, 45, 50, 60, 70, 80, 90, 100, 110, 120, 130, and 140 ms. A minimum 2 ms temporal separation (for the 42 ms delay time) between masker offset and probe onset (each at 10% of peak amplitude) was used in order to minimize physical interactions between masker and probe. For each delay time, the probe was fixed at a level that was approximately 10-dB SL and the masker level was adjusted adaptively to reach the masked threshold for the probe.

Pure tones for the masker and probe stimuli were produced and gated digitally by Tucker Davis Technologies (TDT) D–A converters, routed separately through programmable attenuators, added together in an active mixer, and presented monaurally through a TDH-49 earphone mounted in an MX/AR-1 cushion. Subjects were seated in a double-walled sound-treated booth and conveyed their responses to the computer by pressing buttons on a custom response panel.

A three-interval forced-choice (3IFC) adaptive procedure was used to estimate the masker level needed to just mask the fixed-level probe tones and to measure absolute sensitivity thresholds. During each 3IFC trial, a subject was presented with three observation intervals demarcated by lights. The masker was presented in all three intervals and the probe was presented in only one, randomly selected, interval. The subject indicated which interval contained the probe stimulus by pressing one of three response buttons, after which the correct-answer feedback was given.

Masked thresholds were determined using a transformed up–down adaptive procedure. During the first four level reversals, a relatively large step size of 8 dB and a simple up–down stepping rule were used to move into the target masker-level region. Then a 2-dB step size was used for the next two reversals, again with a simple up–down stepping rule. A 2-up, 1-down, stepping rule, still with the 2 dB step size, was then followed for the final six reversals to estimate the masker level corresponding to 71% correct detection of the probe (Levitt, 1971). Masked threshold was estimated as the mean of the masker levels for the final six reversals. The final data points were based on the average of three or more such thresholds. Standard deviations for the final means were typically under 3 dB. Absolute thresholds for all probes and maskers and for the audiometric frequencies were obtained using a similar 3IFC adaptive procedure that concluded with a 2-down, 1-up stepping rule for the last six level reversals. Final thresholds for the probes and maskers were estimated in the same manner, as were the masked thresholds. The audiograms were based on one threshold estimate.

Two groups of subjects participated in these experiments. Group I consisted of five normal-hearing subjects who were tested at each of six probe frequencies (500, 1000, 2000, 3000, 4000, and 6000 Hz). Their data were used to evaluate the frequency dependence of off-frequency TMC slopes ( $F_m = 0.6F_p$ ), and to obtain a group average off-frequency TMC slope that could be used to calculate compression at all probe frequencies. Group II consisted of nine additional normal-hearing subjects who were tested at one or more probe frequencies that were either 250, 500, 750, 1000, 6000, or 8000 Hz. The average off-frequency TMC slope from Group I was used to calculate compression from the data for each member of Group II. All subjects had absolute thresholds that were 15 dB HL or better (ANSI, 1996) for octave frequencies between 250 and 8000 Hz and at all probe and masker frequencies. All subjects received several hours of practice on forward-masking tasks before data collection commenced.

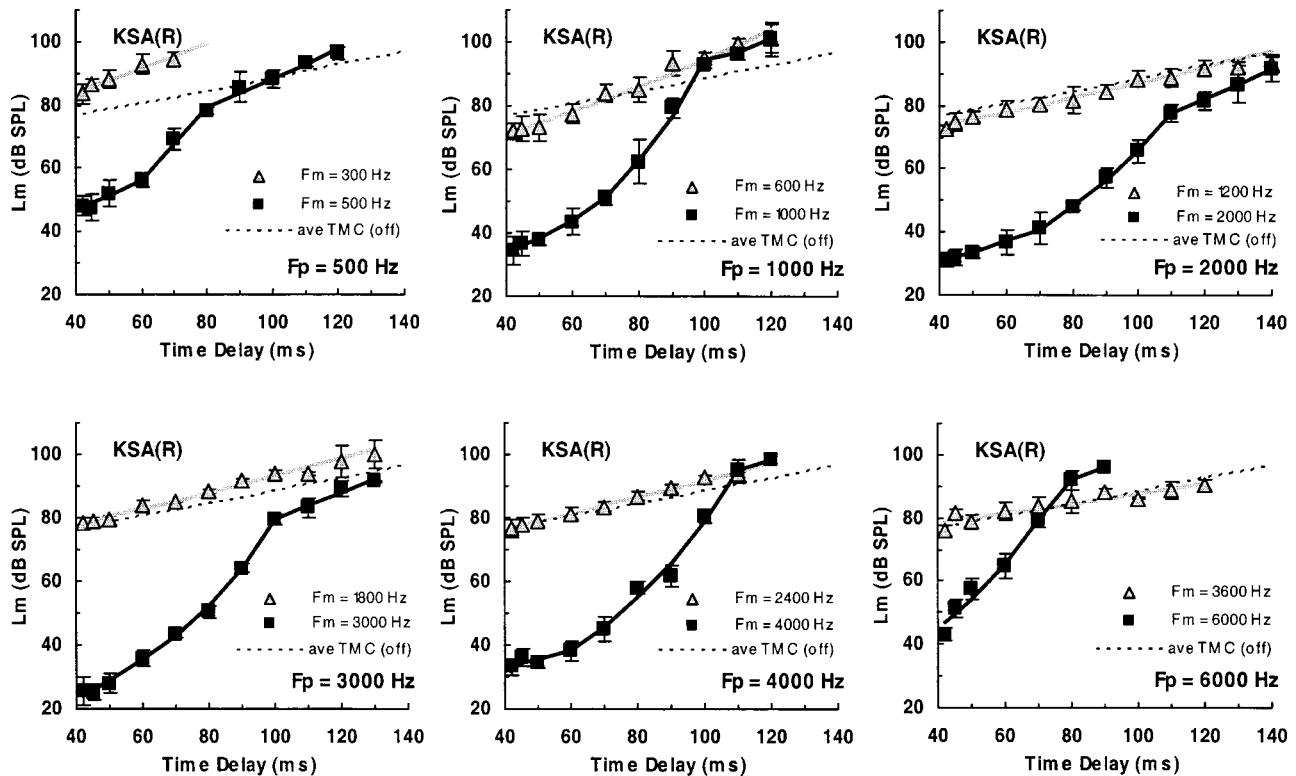


FIG. 1. Temporal masking curves (TMCs) from a normal-hearing subject KSA(R). Each curve shows the masker level required to forward mask a fixed  $\sim 10$ -dB SL probe tone, as a function of the time delay between masker offset and probe offset. Error bars indicate one standard deviation above and below each mean masked threshold. Each panel shows on-frequency ( $F_m = F_p$ ) and off-frequency ( $F_m = 0.6 F_p$ ) TMCs (black squares and shaded triangles, respectively). The black curves are three-segment exponential fits to the on-frequency data. The shaded curves are single-segment exponential fits to the off-frequency data. The dashed curve shows the average off-frequency TMC for probe frequencies from 2–4 kHz in this subject {ave TMC (off)}. Where the slope of a TMC is steeper than the slope for the ave TMC (off), the assumptions underlying the analysis procedures proposed later, indicate that compression exists.

### III. RESULTS

#### A. Fixed-probe-level (isoresponse) TMCs

TMCs obtained at six probe frequencies from one of the normal-hearing listeners in Group I are shown in Fig. 1. Results for this listener exhibit the general effects seen in all of the subjects. The on-frequency TMCs (black squares) tend to reveal a trisegment shape. Slopes are gradual at low masker levels (short time delays), steeper at mid masker levels (medium time delays), and gradually sloped again at high masker levels (longer time delays). The off-frequency TMCs (gray triangles) maintain a relatively constant slope at all masker levels (all time delays).

Using the procedures introduced by Nelson *et al.* (2001), the relative slopes of on-frequency and off-frequency TMCs can be used to estimate compression as a function of input level. Based on the assumption that the off-frequency masker has a linear response at the probe frequency, the slope of the off-frequency TMC reflects only the recovery from forward masking. As time delay increases, the off-frequency masker must be increased to account for more recovery from forward masking. Usually, with the Nelson *et al.* (2001) procedure, the off-frequency TMC is fit (least squares) with a single exponential to provide a continuous specification of TMC slope, as shown by the shaded curves in Fig. 1. Plack and Drga (2003) suggest that at low probe frequencies (250 Hz), the off-frequency TMC is steeper than

at higher frequencies (4000 Hz), and therefore, the off-frequency TMC at low frequencies cannot be used to estimate compression. One explanation for this is that compression extends over a broader *relative* frequency region at low frequencies than at high frequencies. Thus, the off-frequency TMC at low probe frequencies is still influenced by compression. The compression, presumably, increases the TMC slope from what it would be without compression. The fitted off-frequency TMC curves in Fig. 1 (shaded curves) for probe frequencies at 500 and 1000 Hz appear to be steeper than those at higher probe frequencies. To assist this comparison, the dashed line in each panel shows the average of the single exponential fits to the off-frequency TMCs for the 2, 3, and 4 kHz probes obtained from this subject. For this subject, comparisons of individual off-frequency TMCs at each probe frequency (shaded curves) with the average off-frequency TMC (dashed curves) indicates that off-frequency TMCs for probes at 500 and 1000 Hz are slightly steeper than those for probe frequencies at 2000 Hz and higher.

On-frequency TMCs (black squares), in general, exhibit a more complex function. It is assumed that recovery from forward masking is the same with an on-frequency masker as it is with an off-frequency masker. Therefore, if only recovery from forward masking influenced the on-frequency TMC, then the on- and off-frequency TMCs would be parallel but offset to reflect attenuation by the auditory filter.

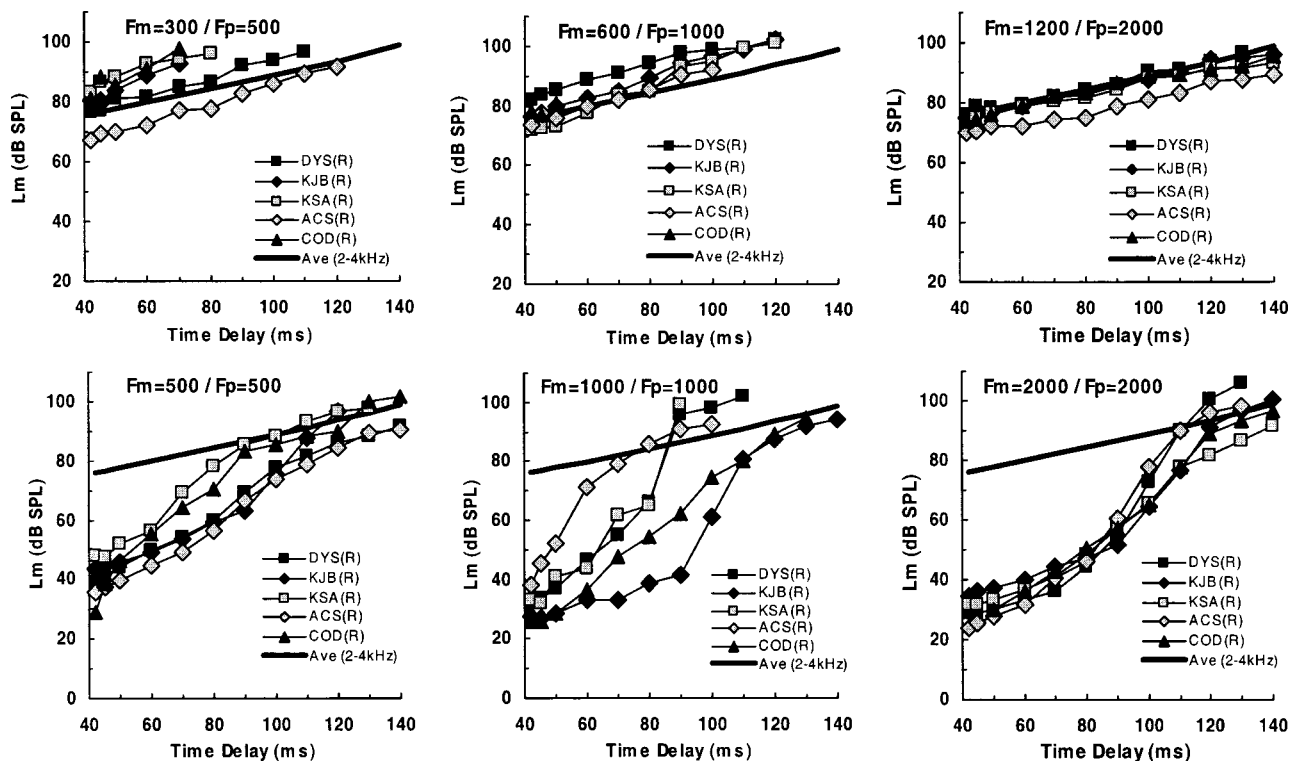


FIG. 2. TMCs from the five Group I subjects for probe frequencies at 0.5, 1.0, and 2.0 kHz. The upper panels show the off-frequency conditions, while the lower panels show the corresponding on-frequency conditions. The *group* average off-frequency TMC {Ave (2–4 kHz)}, shown in each panel by a solid black curve, was based on the average (across the five Group I subjects) of the off-frequency TMCs for probe frequencies from 2000–4000 Hz. This curve was used to derive input/output curves at all probe frequencies.

Thus, the departure of the on-frequency TMC slope from the off-frequency slope reveals the effects of some other process operating on the masker. It is assumed that this process is cochlear compression. As the time delay increases, not only must the masker level increase to account for more recovery from forward masking, but the masker must be increased additionally to overcome the compression imposed on it. The ratio of the slopes of the off-frequency and the on-frequency TMCs at any specific time delay should reveal the magnitude of compression imposed at that particular on-frequency masker level. To aid in the specification of the TMC slope, each of the on-frequency TMCs was fitted with three exponential curves. The fitting procedure was done manually by choosing the number of data points in each segment to minimize differences between fitted and actual data points. However, any fitting procedure that minimizes error would suffice. In general, the fitted curves reveal low-level and high-level segments that are nearly parallel to the off-frequency TMC. The mid-level segment has a steeper slope that reflects the most compression.

Figures 2 and 3 show the off-frequency and on-frequency TMCs obtained from all five subjects in Group I. Each column of panels represents a different probe frequency. On-frequency TMCs are shown in the bottom row of panels in each figure. In general, most on-frequency TMCs exhibit the trisegment form, with individual subject differences in the extent and slope of each segment. Off-frequency maskers are shown in the top row of panels in each figure. All of the off-frequency TMCs were well fit with a single exponential. The solid black curve in each panel shows the

*group* average off-frequency TMC, averaged across all five subjects at probe frequencies from 2–4 kHz {Ave (2–4 kHz)}. Notice that the individual off-frequency TMCs from different subjects are well described by the group average off-frequency TMC curve, except at probe frequencies of 500 and 1000 Hz. At these two probe frequencies, some of the individual curves would be better fit with a steeper function.

## B. Slopes of off-frequency TMCs by probe frequency

Figure 4 shows the fitted off-frequency TMCs at different probe frequencies, for each of the five subjects in Group I. Those TMCs are compared to the *individual* average off-frequency TMC for probe frequencies from 2000–4000 Hz, in each subject, which is shown by the solid curve {Ave TMC (Off)}. Each panel shows this comparison for a different subject. Notice that the fitted TMCs at 500 and 1000 Hz probe frequencies (unfilled symbols) are steeper than the fitted TMCs at higher probe frequencies (filled symbols). This is the case for four of the subjects. Subject ACS exhibited off-frequency TMCs that had essentially the same slopes across probe frequency. Notice also that, for each subject, the Ave TMC (Off) function describes the off-frequency TMC slopes quite well for probe frequencies above 1000 Hz.

From these comparisons, it is clear that fitted off-frequency TMCs for probe frequencies at 500 and 1000 Hz are steeper than they are at higher probe frequencies, for most subjects. This result suggests that off-frequency maskers for probe frequencies at and below 1000 Hz may not

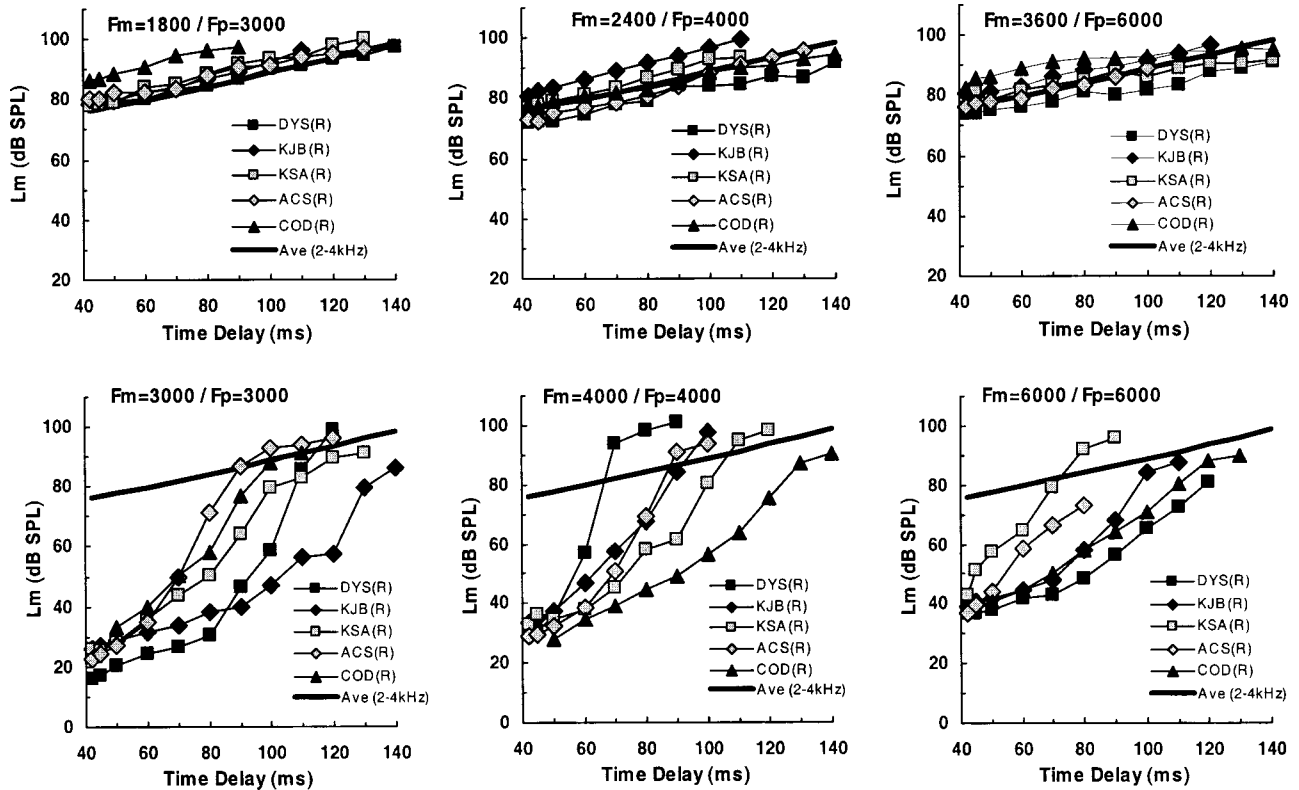


FIG. 3. The same as Fig. 2, but for probe frequencies at 3.0, 4.0, and 6.0 kHz.

exhibit linear response growth at the probe frequency. If this is the case, then the off-frequency TMC slopes for the probe frequencies at 500 and 1000 Hz cannot be used to calculate

compression. As suggested by other investigators (Lopez-Poveda *et al.*, 2003; Plack and Drga, 2003), the off-frequency TMC slope from a higher-frequency region, where

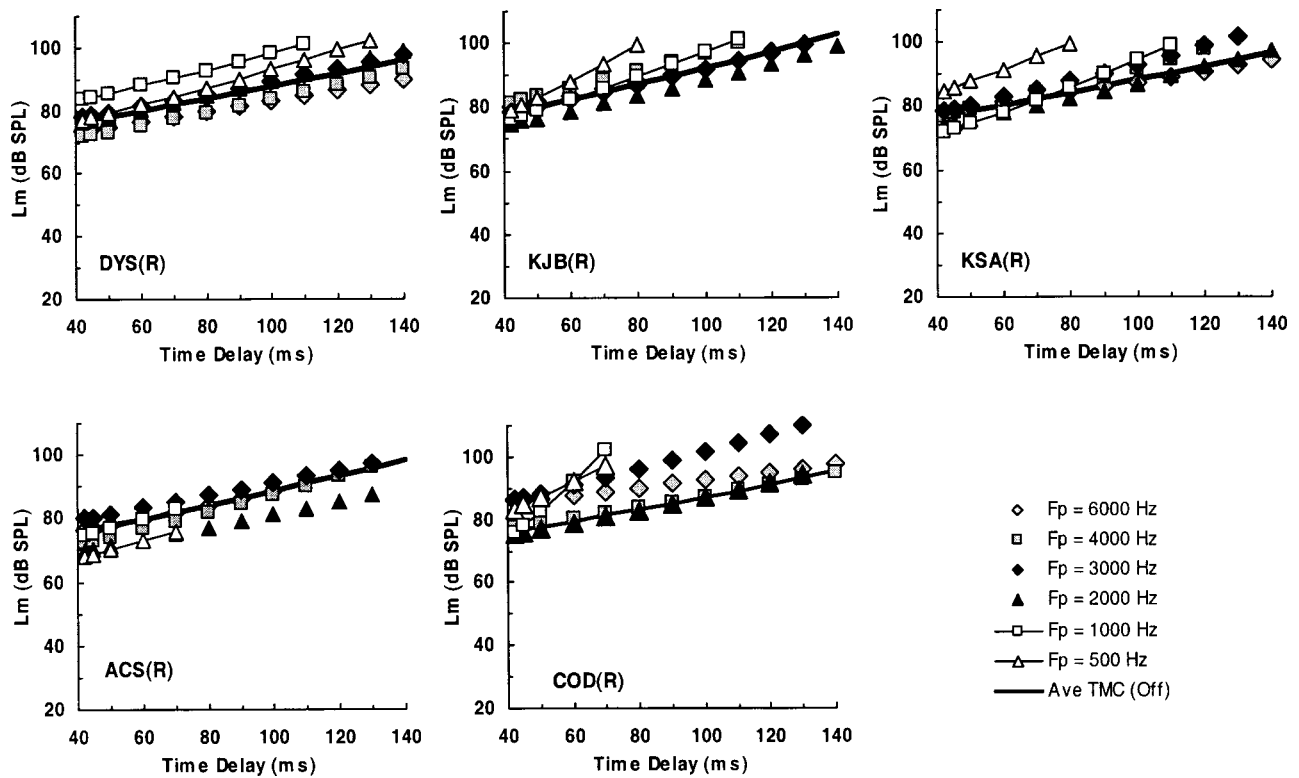


FIG. 4. Off-frequency TMCs ( $F_m = 0.6 F_p$ ) are compared across probe frequencies in the five Group I subjects. The solid black curve in each panel is the average off-frequency TMC at probe frequencies between 2000 and 4000 Hz {ave TMC (Off)} for each individual subject. Probe frequencies at 500 and 1000 Hz, which exhibit steeper off-frequency TMCs, are shown by the open symbols.

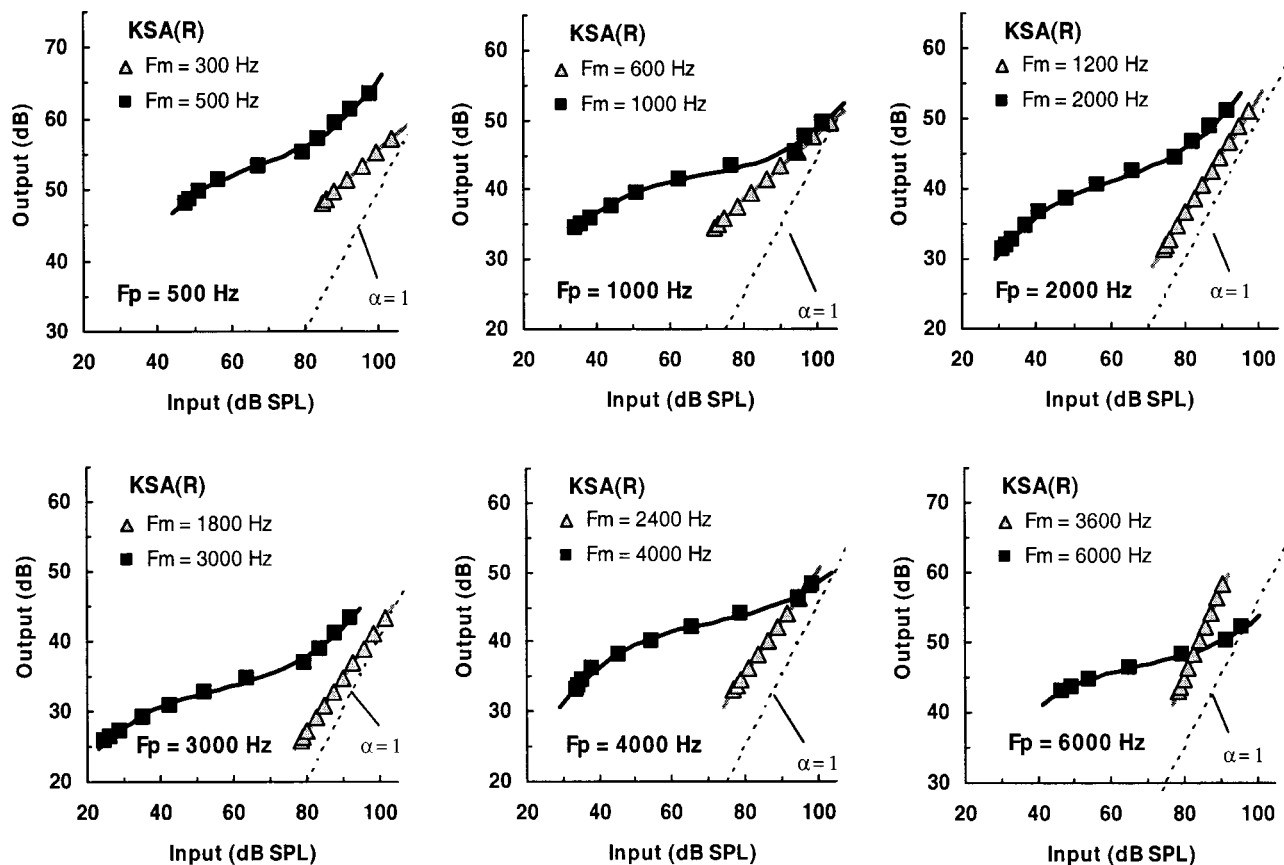


FIG. 5. Input/output curves derived from off-frequency and on-frequency TMCs from subject KSA. On-frequency I/O curves are shown by black squares. Off-frequency I/O curves are shown by shaded triangles. Each panel shows derived I/O curves for a different probe frequency. Note that the origin of the ordinate is 10 dB higher for the 500- and 6000-Hz data. The dotted curve in each graph shows a linear response growth rate ( $\alpha=1$ ), where output (dB) =  $\alpha \times$  input (dB) +  $K$  (an arbitrary constant to adjust the origin on the graph). The solid curves are third-order polynomial fits to the I/O curves, the first derivatives of which were used to specify the response growth rate as a function of input level.

the linearity assumption is more likely to be valid, can be used instead. For the determination of input/output curves and compression characteristics that follow, we used the *group* average off-frequency TMC (shown by the solid curves in Figs. 2 and 3) as the reference from which to calculate off- versus on-frequency TMC slope ratios that specify compression as a function of the input masker level.

### C. Derived I/O curves and compression calculations

Compression was calculated from the TMCs in each subject using the procedures developed by Nelson *et al.* (2001), except for the use of the *group* average 2–4 kHz off-frequency fitted TMC instead of the off-frequency fitted TMC ( $F_m=0.6F_p$ ) associated with each probe frequency. To illustrate this procedure, Fig. 5 shows input/output (I/O) curves derived from TMCs for one of the Group I subjects (KSA). Input levels are the masker levels corresponding to masked thresholds at different time delays, taken from the fitted on-frequency TMC (e.g., solid black curves in Fig. 1). Corresponding output levels are calculated as the changes in input level with time delay, multiplied by estimates of compression. The estimates of compression are usually specified by the ratios between off-frequency and on-frequency fitted TMC slopes, for consecutive time delays (Nelson *et al.*, 2001). However, given the rationale presented above, the *group* average off-frequency TMC ( $F_p=2-4$  kHz) was used

to calculate off- versus on-frequency TMC slope ratios. This also allowed I/O curves to be calculated for the off-frequency conditions at each probe frequency. Thus, in Fig. 5, a linear off-frequency I/O curve with a growth rate of 1.0 ( $\alpha=1$ ) means that the off-frequency TMC for a particular probe frequency had the same slope as the *group* average 2–4 kHz off-frequency TMC curve. Comparisons of the shaded triangles in Fig. 5 with the dotted lines ( $\alpha=1$ ) indicate that off-frequency growth rates at 500 and 1000 Hz were more gradual than at higher probe frequencies.

Our comparisons of off-frequency TMCs at different probe frequencies for Group I subjects revealed consistent differences in off-frequency TMC slopes only at 500 and 1000 Hz. Thus, it is likely that, at those two frequencies, the off-frequency masker response growth was not linear at the probe place, but was subjected to some compression. The effect of this compression is evident in Fig. 4, where the fitted TMCs at 500 and 1000 Hz are steeper than the *individual* average 2–4 kHz off-frequency TMCs in four out of five subjects. This deviation was also apparent in the derived I/O curves for the off-frequency maskers. For example, in Fig. 5, the effects of compression on off-frequency maskers are evident where the derived I/O curves for the off-frequency maskers (shaded triangles) depart from a slope of 1.0 (dashed lines).

The on- frequency I/O curves for subject KSA in Fig. 5

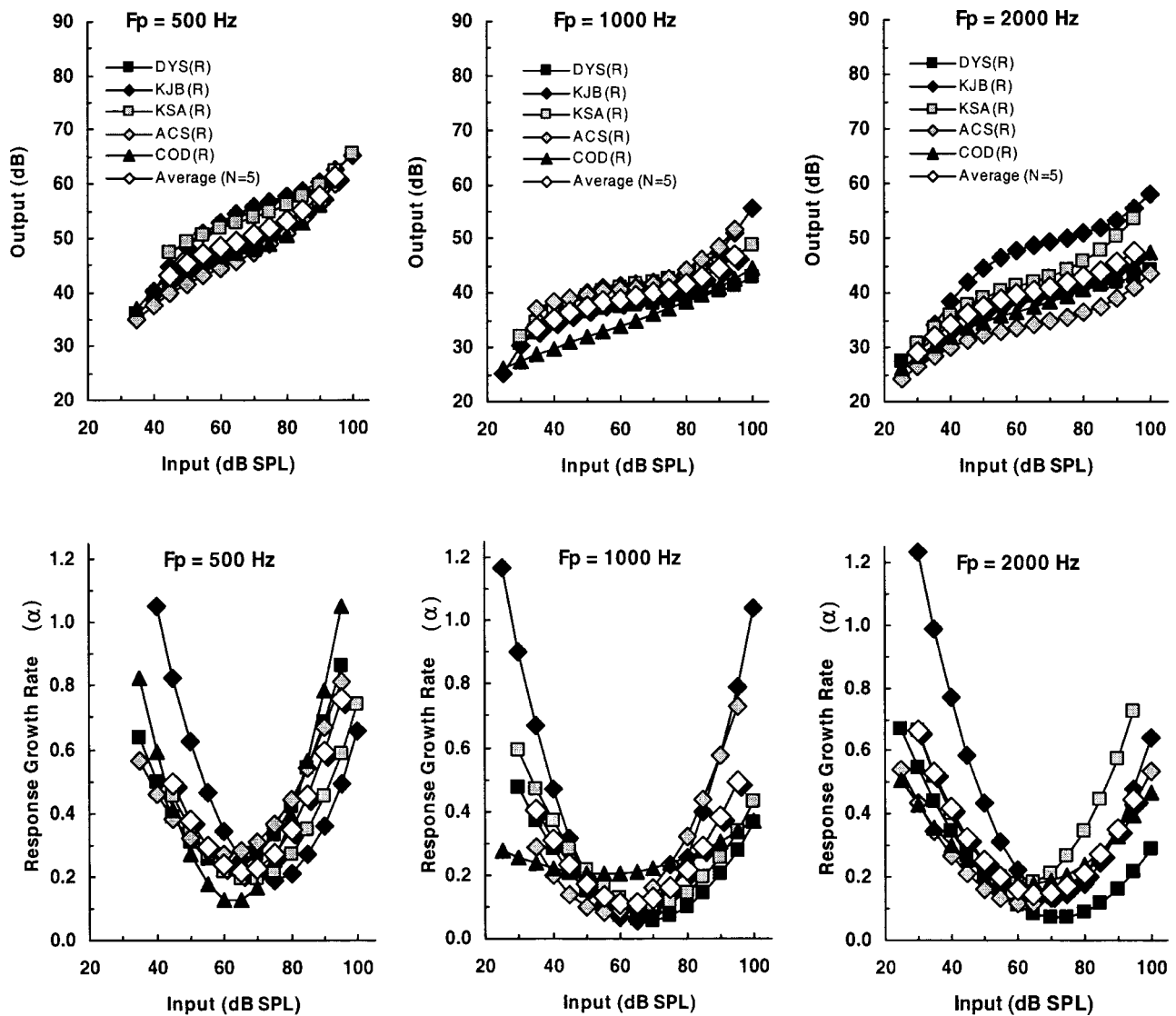


FIG. 6. Input/output response growth curves derived from TMCs (top row), along with response growth rates calculated from the TMCs (bottom row) for the five Group I subjects. Probe frequencies were 500, 1000, and 2000 Hz. Calculations were made at fixed input levels (in 5 dB steps) in order to allow averaging across subjects. Average values, indicated by open symbols, were only calculated at those input levels where data were available from all subjects. The symbols used for the I/O curves in the top row also apply to the response growth rate functions in the bottom row.

(black squares) revealed compression at all six probe frequencies. The general form of every on-frequency I/O curve in this subject was similar, with relatively linear growth for low-level inputs, compressed growth for mid-level inputs, and more linear growth again for high-level inputs. To quantify the magnitude of compression as a function of input level, the derived I/O curves were fitted with a third-order polynomial. In this way the first derivative of the polynomial could be used to specify growth rate (slope of the I/O curve) as a function of input level.

#### D. Comparisons of I/O curves by frequency region

Similar procedures were applied to the TMCs obtained from all subjects. Then, in order to describe the average result across subjects as a function of input level (dB SPL), the derived I/O curves for the on-frequency conditions were recalculated (in 5 dB steps) from the polynomial fits for each subject using the same exact input levels. This facilitated comparisons among subjects at the same input levels for

each probe frequency. It also allowed average I/O curves across subjects to be calculated at each probe frequency to facilitate comparisons of results across frequency regions. Those polynomial fits for the five Group I subjects are shown in Figs. 6 and 7 for different probe frequencies.

The top row of panels in each figure shows the polynomial-fitted I/O curves plotted in 5 dB steps. Averages are shown by unfilled diamonds at each probe frequency. Different probe frequencies are shown in different columns of panels. The bottom row of panels displays the first derivative of the I/O curves, which defines the response growth rate as a function of the input level for each subject. The response growth rate can be interpreted as the compression that exists at any specific input level. All of the growth rate curves are U-shaped, indicating that compression varied continuously with input level. Maximum compression (minimum response growth rate) occurred at moderate input levels (60–70-dB SPL). More linear response growth rates were exhibited at lower and higher input levels.

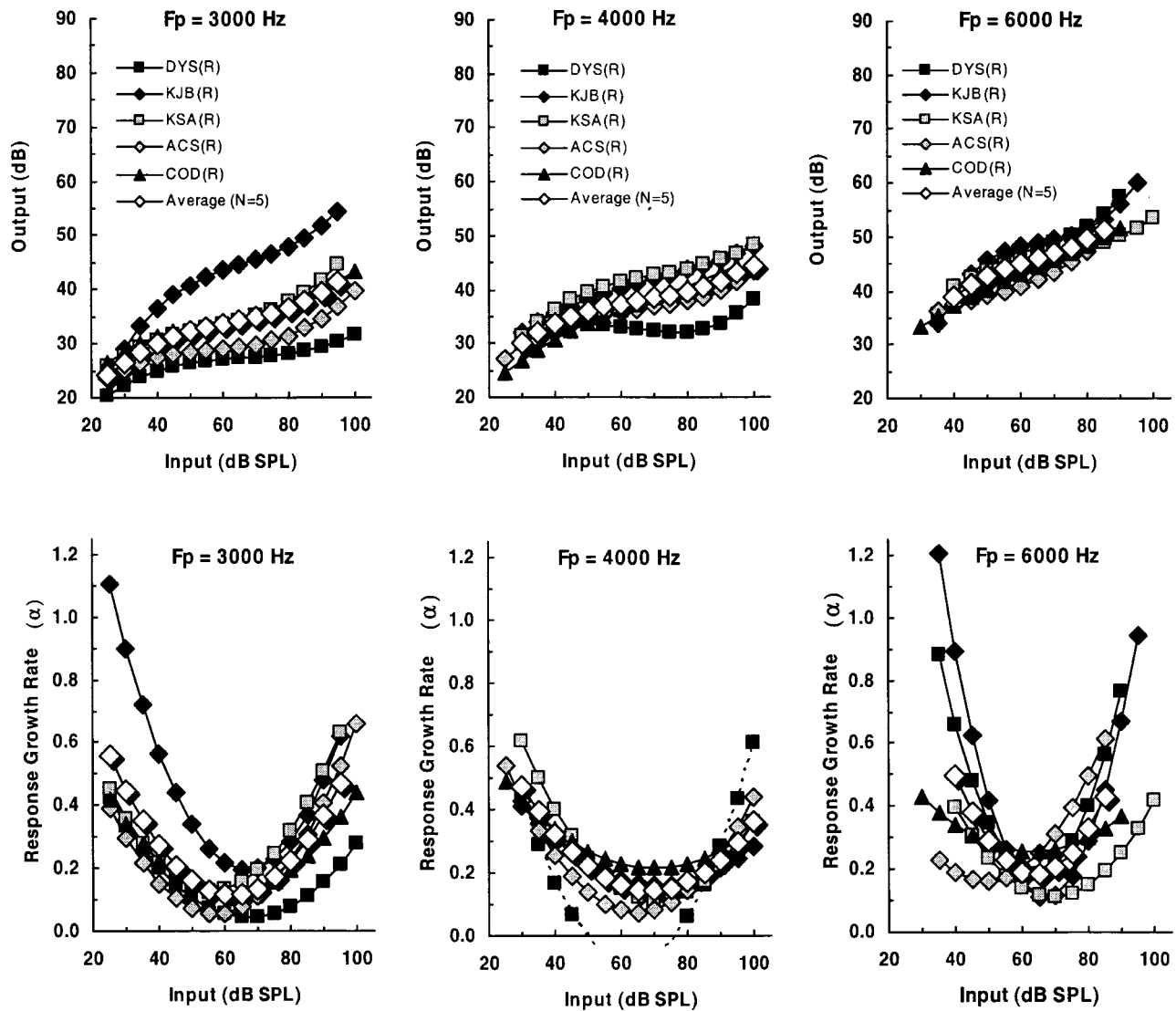


FIG. 7. The same as Fig. 6, but for probe frequencies at 3000, 4000, and 6000 Hz.

Individual differences can be seen among subjects at some frequencies. Those individual differences tended to be larger at lower and higher levels, which can be seen most easily in the U-shaped response growth-rate curves (the bottom row of panels in Figs. 6 and 7). The least variance across subjects occurred in the middle of the input-level range, where compression was the strongest. The negative growth rates at 4000 Hz for subject DYS (black squares with a dashed line) were an artifact of the polynomial fitting procedure; there were no nonmonotonocities in the raw data of the derived I/O curve. The general trends at each probe frequency are summarized by the averaged group curves, shown in Figs. 6 and 7 by the unfilled diamonds. These averages were only calculated at input levels where data existed from all five subjects.

### E. I/O Curves from additional frequency regions

The studies by Hicks and Bacon (1999a), Moore *et al.* (1999), and Plack and Oxenham (2000) suggested that the amount of compression in the auditory system varies depending on the frequency region of the cochlea. However,

the average minimum response growth rates from the Group I subjects did not appear to be particularly higher at 500 Hz than at higher probe frequencies, as would be expected if there were less compression at lower frequencies. Thus, it became apparent that it would be useful to extend the current investigation of compression to lower and higher probe frequencies than originally planned. Subsequently, data from other laboratories suggested that compression might be independent of probe frequency between 250 and 8000 Hz. Plack and Drga (2003) obtained compression estimates in three subjects at 250 Hz, which were not different from those at 4000 Hz. Lopez-Poveda *et al.* (2003) obtained compression estimates in three subjects at 8000 Hz, which were not different from those obtained at lower frequencies.

Because the Group I subjects were not all available for testing at additional probe frequencies, a slightly different experimental design was implemented. Individual subjects were tested at one or more probe frequencies; no attempt was made to test each subject at all probe frequencies. The final sample included nine subjects, with 5, 7, 7, 6, 5 and 4 subjects tested at probe frequencies of 250, 500, 750, 1000, 6000, and 8000 Hz, respectively. Instead of using off-

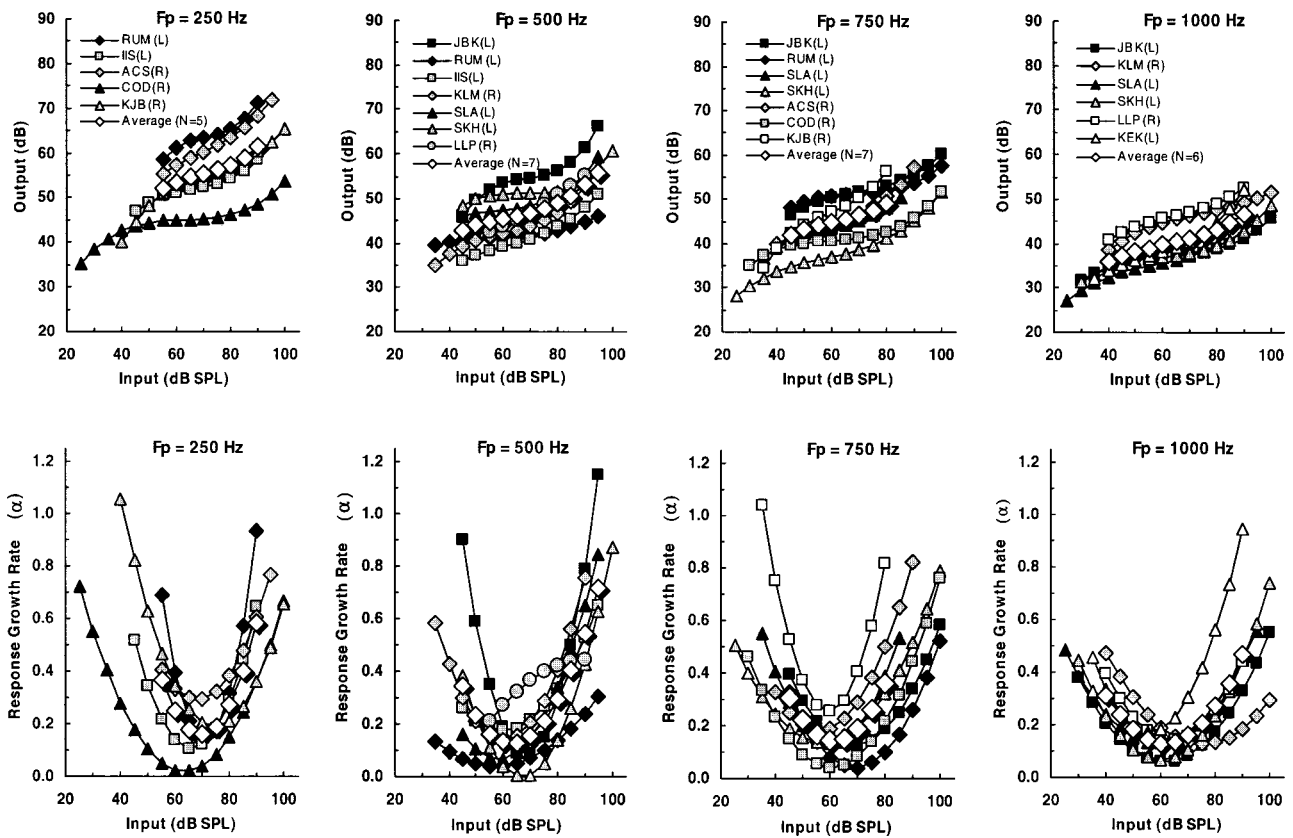


FIG. 8. Input/output response growth curves derived from TMCs (top row), along with response growth rates calculated from the TMCs (bottom row) for Group II subjects. Probe frequencies were 250, 500, 750, or 1000 Hz. Calculations were made at fixed input levels (in 5 dB steps) in order to allow averaging across subjects. Average values, indicated by open diamonds, were only calculated at those input levels where data were available from all subjects. The symbols used for the I/O curves in the top row also apply to the response growth rate functions in the bottom row.

frequency TMCs at each probe frequency, the *group* average 2–4 kHz off-frequency TMC obtained from the Group I subjects was used to calculate compression for these Group II subjects. Although both off-frequency and on-frequency TMCs were obtained from Group II subjects, the results shown here only include derived I/O curves and response growth curves based on the Group II individual on-frequency TMCs and the Group I average 2–4 kHz off-frequency TMC.

The off-frequency TMC slopes from Group II subjects were similar to those obtained from Group I subjects. The 250 Hz off-frequency TMCs were steeper than at higher probe frequencies, but an added complication was encountered with the very high masker levels required to forward mask 250 Hz probe tones. Because probe thresholds were higher at 250 Hz, the masker levels required to mask those probe tones were also higher. Thus, masked thresholds for only the shortest time delays could be obtained before exceeding the limits of the stimulus system at longer time delays. Thus, even if the off-frequency TMC slopes for the 250 Hz probe had been as gradual as at higher probe frequencies, the off-frequency TMC slopes for the 250 Hz probe would have been marginally useful for specifying compression.

Using the same graphical format as in Figs. 6 and 7, Fig. 8 shows derived I/O curves and response-growth estimates obtained from Group II subjects, for probe frequencies between 250 and 1000 Hz. Essentially, the derived I/O curves and response-growth-rate curves for Group II behaved the

same as for Group I. As with the Group I subjects, all of the growth-rate curves were U-shaped, indicating that compression varied continuously with input level. Maximum compression (minimum response growth rate) occurred at moderate input levels (60–70-dB SPL); response growth rates at lower and higher input levels were more linear. At the 250 Hz probe frequency, the I/O curves exhibited slightly higher output levels, which was due primarily to higher absolute thresholds at 250 Hz than at the higher frequencies. The response-growth rates were just as steep as at higher probe frequencies, but the range over which strong compression occurred was slightly smaller at 250 Hz than at higher frequencies.

Figure 9 shows derived I/O curves and response growth estimates obtained from the Group II subjects who were tested at a probe frequency of 6000 or 8000 Hz. At these high frequencies, I/O curves were similar to those observed at lower probe frequencies, with near linear growth at low and high input levels and compressive growth at mid-input levels. Response growth rate curves were U-shaped with maximum compression (minimum growth rates) at mid-levels. One subject (KSA) was more sensitive at 8000 Hz than the other three subjects, so data from that subject were not included in calculation of the average curve shown in Fig. 9.

To compare results across frequency regions more easily, the across-subject averaged results for Group I and Group II subjects are replotted in Fig. 10. Several general

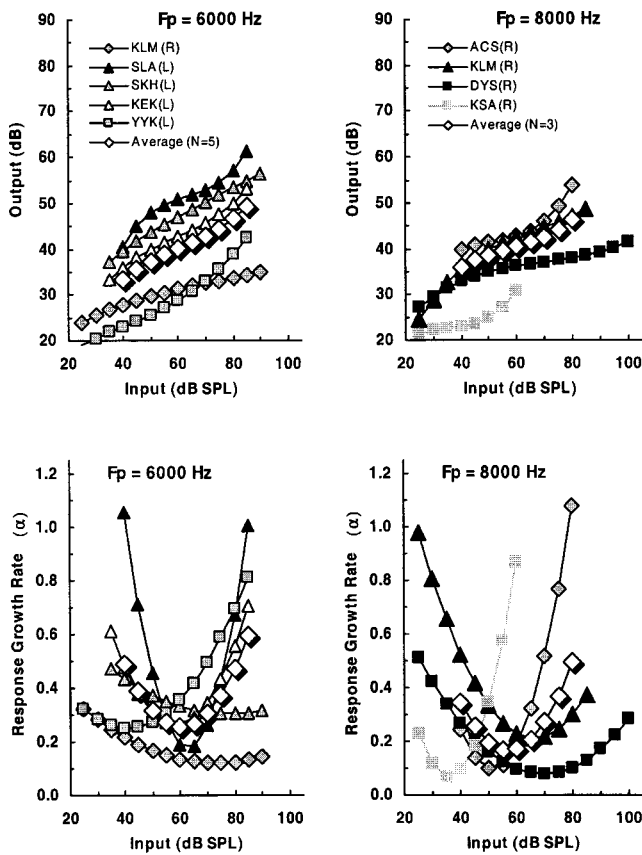


FIG. 9. The same as Fig. 8, but for probe frequencies at 6000 and 8000 Hz. Subject KSA was not included in the average at 8000 Hz.

findings are apparent in this figure. Output levels were slightly higher at 250, 500, 750, and 6000 Hz probe frequencies (top panels), primarily because probe thresholds were higher at these frequencies. Since the lowest output level was always the on-frequency masker level at the shortest time delay (42 ms), higher probe thresholds required higher probe levels, which required higher masker levels. Compression was the strongest (lowest response growth rates) for input levels between 60- and 70-dB SPL, regardless of probe frequency. Strong compression was limited to a slightly smaller range of input levels at 250, 500, 6000, and 8000 Hz, which can be seen by their slightly narrower U-shaped response growth-rate functions (bottom panels).

### F. Comparisons of maximum compression by frequency region

In order to compare compression across probe frequency regions, the minimum response growth rate, estimated across all input levels, was estimated for each subject at each probe frequency (minimums in the growth-rate versus input-level curves in Figs. 6, 7, 8, and 9). The average minimum response growth-rate (across subjects) then provides an estimate of the maximum compression seen at each probe frequency. Figure 11 shows the average minimum response growth rate for Group I subjects (unfilled squares) and Group II subjects (unfilled triangles) as a function of probe frequency.

An examination of the results in Fig. 11 (unfilled squares and triangles) indicates that the average minimum growth

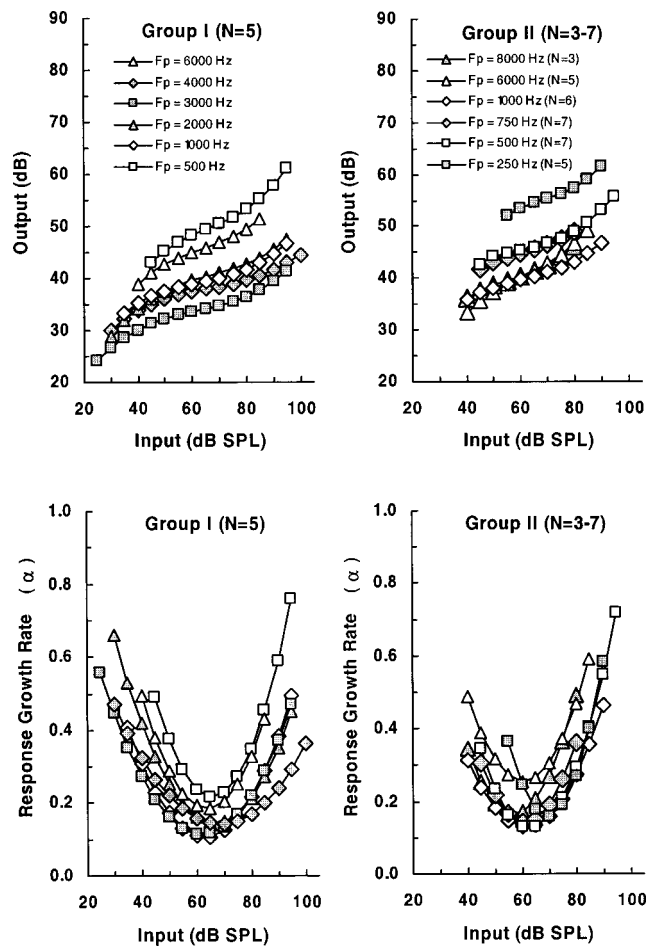


FIG. 10. Across-subject average input/output response growth curves derived from TMCs (top panels), along with average response growth rates (bottom panels) calculated from the TMCs from Group I subjects (left panels) and Group II subjects (right panels). The parameter is probe frequency.

rate does not vary noticeably across probe frequency region. The average minimum growth rate at each probe frequency for Group I subjects (unfilled squares) varied between 0.10 and 0.20 (see Table I). A single-factor ANOVA of Group I results showed that there were no significant differences in average minimum growth rates across probe frequency ( $p > 0.10$ ). The average minimum growth rate at each probe frequency from Group II subjects (unfilled triangles) varied between 0.10 and 0.22 (see Table I). When the two groups were combined, the average response growth rate ranged between 0.11 and 0.20 at different probe frequencies, with a grand mean of 0.14 across subjects and probe frequencies (solid line in Fig. 11). Regression analysis of the averaged minimum response growth rates yielded a nonsignificant trend across probe frequency ( $p > 0.69$ ;  $R^2 = 0.02$ ). Thus, the average minimum growth rate appears to be independent of probe frequency. At its maximum along the I/O curve, compression is equally strong at all frequency regions.

## IV. DISCUSSION

The major finding of this study, that compression is relatively constant across probe frequency regions, differs from some previous psychophysical estimates of compression that utilized on- versus off-frequency growth-of-masking slope

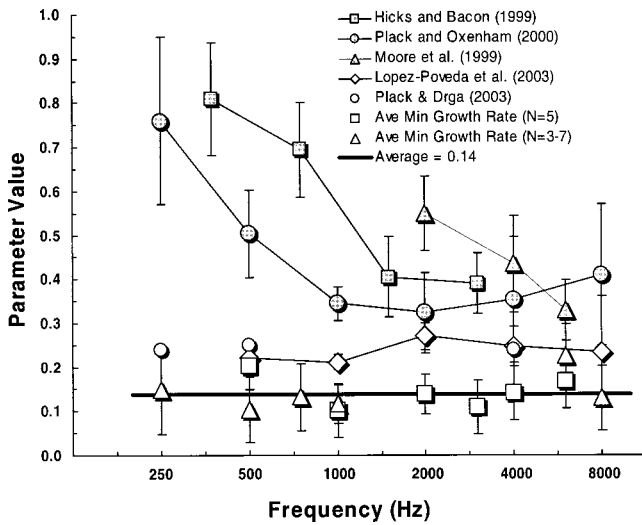


FIG. 11. The average *minimum* growth rates (maximum compression) obtained in the current experiment are shown by the unfilled squares (Group I) and the unfilled triangles (Group II) as a function of probe frequency. Error bars are standard deviations about the mean values. Average minimum growth rate across *all* subjects and probe frequencies is shown by the solid line. Response growth rates estimated by Lopez-Poveda *et al.* (2003) and by Plack and Drga (2003) with similar TMC experiments are shown by the unfilled diamonds and circles, respectively. These investigations used off-frequency TMCs from high-frequency probes as a reference for estimating compression. Response growth rate estimates obtained from *slope ratios* between on-frequency and off-frequency nonsimultaneous-masking functions are shown by the shaded symbols. Slope ratios between on- and off-frequency growth-of-forward-masking functions reported by Hicks and Bacon (1999a) and by Moore *et al.* (1999) are shown by shaded squares and shaded triangles, respectively. Slopes of growth-of-maskability pulsation-threshold functions (masker level versus probe level) from Plack and Oxenham (2000) are shown by shaded circles.

ratios to estimate compression. The filled symbols in Fig. 11 show compression estimates obtained by previous investigations using nonsimultaneous masking (Moore *et al.*, 1999; Hicks and Bacon, 1999a; Plack and Oxenham, 2000). There are two obvious differences between those results and the current estimates. First, at all probe frequencies, the previous estimates (shaded symbols) are larger than the current estimates (unfilled symbols), i.e., the previous methods underestimated the strength of compression. Second, the previous estimates become larger as probe frequency is reduced below 1000 Hz, i.e., the previous estimates indicated that compression is less strong at lower probe frequency regions. The first effect is probably due to off-frequency listening. The second is probably due to an invalid assumption about linear response growth for off-frequency maskers at low probe frequencies. Our reasoning for these conclusions follows.

## A. Off-frequency listening effects

Previous estimates of compression shown in Fig. 11 involved the acquisition of growth-of-masking (GOM) functions for nonsimultaneous masker and probe tones. Two of the investigations involved forward masking (Moore *et al.*, 1999; Hicks and Bacon, 1999a), and one involved the pulsation threshold (Plack and Oxenham, 2000). These estimates of compression were derived from GOM slope ratios for on-frequency and off-frequency nonsimultaneous maskers, which were presented in a quiet background. The rationale for using this GOM slope ratio to estimate compression came from an experiment by Oxenham and Plack (1997), in one subject, in which they found that the GOM slope ratio in quiet was similar to the GOM slope ratio obtained in a background noise that masked off-frequency listening (Patterson and Nimmo-Smith, 1980; O'Loughlin and Moore, 1981; Yacullo and Abbas, 1986). Presumably off-frequency listening that affected the on-frequency GOM slope had a similar effect on the off-frequency GOM slope. Thus, the ratio between on-frequency and off-frequency GOM slopes evolved as a psychophysical estimate of compression.

For these previous estimates of compression, both the masker level and probe level covaried in a quiet background; either the probe level at masked threshold increased with masker level (Hicks and Bacon, 1999a) or the masker level at masked threshold increased with probe level (Moore *et al.*, 1999; Plack and Oxenham, 2000). When both masker and probe level co-vary, off-frequency listening can dramatically affect GOM slopes (Bacon *et al.*, 1999; Plack and Oxenham, 2000; Nelson *et al.*, 2001). This phenomenon has been confirmed by the introduction of a high-pass noise above the probe frequency to restrict "listening" only to frequency regions near the probe frequency (Oxenham and Plack, 1997; Plack and Oxenham, 2000; Nelson *et al.*, 2001). Specifically, Nelson *et al.* found that GOM slopes increased in the presence of a high-pass noise, more so for an off-frequency masker than for an on-frequency masker. Compression estimates were based on the slope ratios between on-frequency and off-frequency GOM functions, as was the case with the previous compression estimates noted above (Moore *et al.*, 1999; Hicks and Bacon, 1999a; Plack and Oxenham, 2000). Compression estimates were underestimated (slope ratios were larger) by about a factor of 2.3, when GOM functions were obtained in a quiet background that allowed off-frequency listening to take place (slope ratios of 0.26 and 0.35 from two subjects), than when GOM functions were obtained in a high-pass noise that restricted off-frequency

TABLE I. Average minimum response growth rates (and standard deviations) at different probe frequencies for two groups of normal-hearing listeners. Group I includes five subjects tested at each of six probe frequencies. Group II includes nine subjects tested at one or more probe frequencies.

	Probe frequency								
	250	500	750	1000	2000	3000	4000	6000	8000
Group I ( <i>N</i> = 5)		0.20		0.10	0.14	0.11	0.14	0.17	
Stdev		0.055		0.060	0.046	0.061	0.061	0.060	
Group II	0.15	0.10	0.13	0.12				0.22	0.13
Stdev	0.101	0.074	0.076	0.044				0.072	0.073
<i>N</i> =	5	7	7	6				5	3

listening (slope ratios of 0.11 and 0.16) (Nelson *et al.*, 2001).

It is notable that the previous estimates of compression at 1000 Hz and above, in Fig. 11, differ from the current estimates of compression, by a factor of approximately 2.5. Those previous estimates involved GOM functions in which both the masker and probe covaried, without any background noise to restrict off-frequency listening. The current estimates of compression were obtained with a technique that does not allow the probe level to vary, and thus is not influenced substantially by off-frequency listening. This was previously confirmed by Nelson *et al.* (2001) with TMCs obtained in the presence of a high-pass noise. These comparisons strongly suggest that the underestimation of compression by a factor of about 2.5 by the previous investigations was very likely due to off-frequency listening.

## B. Linearity assumptions for off-frequency maskers

Regardless of issues relating to off-frequency listening, the GOM slope ratio estimates of compression are strongly dependent on the off-frequency GOM slope. For example, if compression affects the off-frequency masker response growth, at the on-frequency place, then the GOM slope for the off-frequency masker will be more gradual, and the subsequent on- versus off-frequency GOM slope-ratio will be larger, which will be interpreted as less compression. This is essentially the result exhibited in Fig. 11 by the previous estimates of compression across the probe frequency region. In two of the previous studies (Hicks and Bacon, 1999a; Plack and Oxenham, 2000), response growth rates increased with decreasing probe frequency for probe frequencies below 1000 Hz; in the other study (Moore *et al.*, 1999), response growth rates decreased progressively as probe frequency decreased from 6000 to 2000 Hz. These results are consistent with the idea proposed by Plack and Drga (2003) and Lopez-Poveda *et al.* (2003) that the masker response at the probe frequency, for a fixed Fm/Fp ratio, is less linear at lower frequency regions. Thus, estimates of compression taken from on- versus off-frequency GOM slope ratios appear to be less at low frequencies.

By way of contrast, the estimates of compression shown by unfilled symbols in Fig. 11 did not change significantly with the probe frequency region. Compression estimates from the current study are shown by the unfilled squares and triangles. Similar data from Lopez Poveda *et al.* (2003) and Plack and Drga (2003) are shown by the unfilled diamonds and circles, respectively. The similarity was largely because neither estimate of compression depended upon the assumption of linear response growth for the off-frequency maskers at lower probe frequencies.

The average compression estimates obtained by Lopez-Poveda *et al.* (2003) and Plack and Drga (2003) ranged between 0.21 and 0.27, while the estimates from the current study ranged between 0.10 and 0.22 (average=0.14). Their compression estimates were independent of probe frequency, as in the current study, but the compression estimates were less strong (steeper response growth rates) than the current estimates. The reason for this difference is most likely found in slight differences in the procedures used to estimate response growth rates from derived I/O curves. For example,

Lopez-Poveda *et al.* fitted their derived I/O curves with up to three linear segments. The slope of a mid-range segment was used to estimate compression. The number of input levels included in that mid-range segment varied among subjects, but often included a wide range of input levels. By contrast, the current procedure fitted derived I/O curves with a third-order polynomial, which presumes that compression changes continuously with input level, and allows one to calculate compression continuously along the derived I/O curve. Specification of the *minimum* response growth rate with this procedure leads to more gradual slope estimates, largely because it does allow specification of local response growth rates. Had the current study averaged local compression over a range of input levels, the amount of compression would have been less (larger response growth rates) and more in line with estimates obtained by Lopez-Poveda *et al.* and Plack and Drga (2003). Regardless, all three studies found that their compression estimates were independent of the probe frequency region.<sup>2</sup>

## V. SUMMARY AND CONCLUSIONS

Response growth rates obtained with isoresponse TMCs vary continuously with the input level from near linear at low levels, to highly compressive at mid-levels, to near linear again at high levels. Derived I/O curves are similar across probe frequency regions from 250 to 8000 Hz, as long as the average off-frequency TMC for high probe frequencies (2000–4000 Hz) is used to derive those growth rates. The minimum response growth rate (maximum compression) tends to remain the same at all probe frequencies, but the range of input levels with strong compression is slightly smaller at lower and higher frequencies. Compression estimates obtained by some investigators, using slope ratios between on-frequency and off-frequency nonsimultaneous GOM functions, underestimated maximum compression. In addition, those studies also underestimated compression at lower-frequency regions, largely because they relied on the assumption of linear response growth at the probe frequency for off-frequency maskers.

## ACKNOWLEDGMENTS

This work was supported largely by Grant No. DC00149 from NIDCD. This research was also supported in part by the Lion's 5M International Hearing Foundation. The authors appreciate the excellent suggestions to this manuscript provided by Sid Bacon and Chris Plack.

<sup>1</sup>The TMC procedure for estimating compression was first introduced at a special session honoring the contributions of Robert C. Bilger: "Bilger and Better Science" [Nelson, D.A. and Schroder, A.C. (1999). "Forward masking recovery and peripheral compression in normal-hearing and cochlear-impaired ears," J. Acoust. Soc. Am. **106**, 2176(A)]. That presentation acknowledged Bob's strong influence on current research in the field, particularly on the search for measures of nonlinearity in normal and impaired ears.

<sup>2</sup>As pointed out by previous investigators (Plack and Drga (2003) and Plack and O'Hanlon (2003)), compression at low-frequency regions indicated by psychophysical measurements could well have a central origin.

- Bacon, S. P., Boden, L. N., Lee, J., and Repovsch, J. L. (1999). "Growth of simultaneous masking for fm < fs: Effects of overall frequency and level," *J. Acoust. Soc. Am.* **106**, 341–350.
- Cooper, N. P., and Rhode, W. S. (1995). "Nonlinear mechanics at the apex of the guinea-pig cochlea," *Hear. Res.* **82**, 225–243.
- Cooper, N. P., and Yates, G. K. (1994). "Nonlinear input–output functions derived from the responses of guinea-pig cochlear nerve fibers: Variations with characteristic frequency," *Hear. Res.* **78**, 221–234.
- Hicks, M. L., and Bacon, S. P. (1999a). "Psychophysical measures of auditory nonlinearities as a function of frequency in individuals with normal hearing," *J. Acoust. Soc. Am.* **105**, 326–338.
- Hicks, M. L., and Bacon, S. P. (1999b). "Effects of aspirin on psychophysical measures of frequency selectivity, two-tone suppression, and growth of masking," *J. Acoust. Soc. Am.* **106**, 1436–1451.
- Khanna, S. M., and Hao, L. F., (1999). "Nonlinearity in the apical turn of living guinea pig cochlea," *Hear. Res.* **135**, 89–104.
- Levitt, H. (1971). "Transformed up-down methods in psychoacoustics," *J. Acoust. Soc. Am.* **49**, 467–477.
- Lopez-Poveda, E. A., Plack, C. J., and Meddis, R. (2003). "Cochlear nonlinearity between 500 and 8000 Hz in listeners with normal hearing," *J. Acoust. Soc. Am.* **113**, 951–960.
- Moore, B. C. J., and Oxenham, A. J. (1998). "Psychoacoustic consequences of compression in the peripheral auditory system," *Psychol. Rev.* **105**, 108–124.
- Moore, B. C. J., Vickers, D. A., Plack, C. J., and Oxenham, A. J. (1999). "Inter-relationship between different psychoacoustic measures assumed to be related to the cochlear active mechanism," *J. Acoust. Soc. Am.* **106**, 2761–2778.
- Murugasu, E., and Russell, I. J. (1995). "Salicylate ototoxicity: The effects on basilar membrane displacement, cochlear microphonics, and neural responses in the basal turn of the guinea pig cochlea," *Aud. Neurosci.* **1**, 139–150.
- Nelson, D. A., and Freyman, R. L. (1987). "Temporal resolution in sensorineural hearing-impaired listeners," *J. Acoust. Soc. Am.* **81**, 709–720.
- Nelson, D. A., and Schroder, A. C., (1997). "Linearized response growth inferred from growth-of-masking slopes in ears with cochlear hearing loss," *J. Acoust. Soc. Am.* **101**, 2186–2201.
- Nelson, D. A., Schroder, A. C., and Wojtczak, M. (2001). "A new procedure for measuring peripheral compression in normal-hearing and hearing-impaired listeners," *J. Acoust. Soc. Am.* **110**, 2045–2064.
- O'Loughlin, B. J., and Moore, B. C. J. (1981). "Off-frequency listening: Effects on psychoacoustical tuning curves obtained in simultaneous and forward masking," *J. Acoust. Soc. Am.* **69**, 1119–1125.
- Oxenham, A. J., and Plack, C. J. (1997). "A behavioral measure of basilar-membrane nonlinearity in listeners with normal and impaired hearing," *J. Acoust. Soc. Am.* **101**, 3666–3675.
- Patterson, R. D., and Nimmo-Smith, I. (1980). "Off-frequency listening and auditory-filter asymmetry," *J. Acoust. Soc. Am.* **67**, 229–245.
- Plack, C. J., and Drga, V. (2003). "Psychophysical evidence for auditory compression at low characteristic frequencies," *J. Acoust. Soc. Am.* **113**, 1574–1586.
- Plack, C. J., and O'Hanlon, C. G. (2003). "Forward masking additivity and auditory compression at low and high frequencies," *J. Assoc. Res. Otolaryngol.* **4**, 405–415.
- Plack, C. J., and Oxenham, A. J. (2000). "Basilar-membrane nonlinearity estimated by pulsation threshold," *J. Acoust. Soc. Am.* **107**, 501–507.
- Rhode, W. S., and Cooper, N. P. (1996). "Nonlinear mechanics in the apical turn of the chinchilla cochlea *in vivo*," *Aud. Neurosci.* **3**, 101–121.
- Rhode, W. S., and Recio, A. (2000). "Study of mechanical motions in the basal region of the chinchilla cochlea," *J. Acoust. Soc. Am.* **107**, 3317–3332.
- Rhode, W. S., and Robles, L. (1974). "Evidence from Mossbauer experiments for nonlinear vibration in the cochlea," *J. Acoust. Soc. Am.* **55**, 588–596.
- Robles, L., Ruggero, M. A., and Rich, N. C. (1986). "Basilar membrane mechanics at the base of the chinchilla cochlea. I. Input-output functions, tuning curves, and response phases," *J. Acoust. Soc. Am.* **80**, 1364–1374.
- Ruggero, M. A. (1992). "Responses to sound of the basilar membrane of the mammalian cochlea," *Curr. Opin. Neurobiol.* **2**, 449–456.
- Ruggero, M. A., Rich, N. C., Recio, A., Narayan, S. S., and Robles, L. (1997). "Basilar-membrane responses to tones at the base of the chinchilla cochlea," *J. Acoust. Soc. Am.* **101**, 2151–2163.
- Russell, I. J., and Nilsen, K. E. (1997). "The location of the cochlear amplifier: Spatial representation of a single tone on the guinea pig basilar membrane," *Proc. Natl. Acad. Sci. U.S.A.* **94**, 2660–2664.
- Yacullo, W. S., and Abbas, P. J. (1986). "Detection cues in forward masking and their relationship to off-frequency listening," *J. Acoust. Soc. Am.* **80**, 452–465.
- Yates, G. K. (1990). "Basilar membrane nonlinearity and its influence on auditory nerve rate-intensity functions," *Hear. Res.* **50**, 145–162.
- Yates, G. K., Winter, I. M., and Robertson, D. (1990). "Basilar membrane nonlinearity determines auditory nerve rate-intensity functions and cochlear dynamic range," *Hear. Res.* **45**, 203–219.
- Zinn, C., Maier, H., Zenner, H.-P., and Gummer, A. W. (2000). "Evidence for active, nonlinear, negative feedback in the vibration response of the apical region of the *in-vivo* guinea-pig cochlea," *Hear. Res.* **142**, 159–183.